Goddard Convective-Stratiform Heating (CSH) Algorithm

Wei-Kuo Tao and Steve Lang

Latent heating (LH) cannot be measured directly with current techniques, including current remote sensing or *in situ* instruments, which explains why nearly all satellite retrieval schemes depend heavily on some type of cloud-resolving model or CRM (Tao *et al*. 2006, 2016). This is true for the current CSH algorithm (Tao et al. 2010).

Input: Combined 2BCMB (DPR + GMI) rainfall products

The CSH algorithm only requires information on surface precipitation rates, amount of stratiform rain, and the location of the observed cloud systems (i.e., land or ocean).

Look-Up Tables (LUTs):

The CSH products are based on heating look-up tables (LUTs). The LUTs are generated from a high-resolution CRM (i.e., the Goddard Cumulus Ensemble model or GCE), which can simulate surface rainfall and Q_1 profiles (i.e., LH+Eddy+Qr) that are in very good agreement with sounding estimates.

LUTs derived from multi-week CRM (i.e., GCE) simulations are composited into land and ocean regions. Each set of land/ocean LUTs consists of stored mean latent, radiative and eddy-heating profiles separated into **conditional surface rain intensity** (please see Figure 1) **and stratiform fraction bins** (please see the examples shown in Figure 2). However, the current LUTs are only based on a limited number of cases (i.e., several tropical oceanic but only a couple continental; please see Table 1). **That is why CSH (and SLH) products are only being produced over the TRMM domain for GPM.** Please see Tao et al. (2010) for a description of the current version of the Goddard CSH algorithm. Please also note that for the current GPM version, the 2BCMB input data are first center smoothed to make them compatible with the current CSH LUTs, which were originally designed for the 0.5 x 0.5 degree TRMM grids. The pixel product is not smoothed and only uses the most convective or most stratiform LUT bins as each rain pixel is either convective or stratiform.

Products:

Level 2: Latent heating pixel orbital data (2HCSH, quasi-standard)
Level 3: Latent heating 0.25 degree gridded orbital (3GCSH)
Level 3: Latent heating 0.25 degree gridded monthly (3HCSH)

Each product contains LH, eddy heating, radiative heating, microphysical moistening and eddy moistenting.

Resolution:

Level 2: 5 km horizontal, 19 vertical levels (same as TRMM CSH 2B31 L2)

Level 3: 0.25 degree horizontal, 19 vertical levels (same vertical as TRMM CSH 2B31 L3 but with 0.25 degree versus 0.5 degree horizontal resolution)

Caveats:

The CSH-derived heating profiles are sensitive to DPR/GMI-derived surface rainfall (affects the magnitude) and stratiform percentage (affects the vertical distribution and level of peak heating).

The CSH latent heating profiles are also sensitive to the LUTs. However, the current LUTs are only based on a limited number of cases (several tropical oceanic but only a couple continental; please see Table 1).

Next GPM LH Products:

The LUTs need to include cases associated with fronts and snow events, including mid-latitude synoptic and winter storms. Theses same cases will also be used to generate the LUTs needed for the SLH algorithm**. LH products covering the entire GPM domain are expected to be released starting in December 2016.**

Field Campaign	*Geographic Location*	*Starting Date*	*Modeling Days*	
ARM-SGP-97	(37°N, 97°W)	18 Jun 1997	29	Tao *et al.* (2004); Zeng *et al.* (2009)
ARM-SGP-02		25 May 2002	20	Zeng *et al.* (2007, 2009)
SCSMEX/NESA	(21°N, 117°E)	6 May 1998	44	Tao *et al.* (2003b), Zeng *et al.* (2008)
TOGA-COARE	(2°S, 154°E)	1 Nov 1992	61	Das *et al*. (1999); Johnson *et al*. (2002); Zeng *et al.* (2009)
GATE	(9°N, 24°W)	1 Sep 1974	18	Li *et al.* (2002); Zeng *et al*. (2009)

Table 1: Field campaigns (ARM, SCSMEX, TOGA COARE and GATE) used to build the current CSH LUTs including their geographic location, starting time and length of integration for the corresponding GCE model simulations. Also listed are the GCE modeling papers that have simulated the case.

References:

Das, S., D. Johnson and W.-K. Tao, 1999: Single-column and cloud ensemble model simulations of TOGA COARE convective systems, *J. Meteor. Soc. Japan*, 77, 803-826.

Johnson, D. E., W.-K. Tao, J. Simpson, and C.-H. Sui, 2002: A study of the response of deep tropical clouds to large-scale thermodynamic forcing. Part I: Modeling strategies and simulations of TOGA COARE convective systems. *J. Atmos. Sci.*, **59**, 3492-3518.

Tao, W.-K., C.-L. Shie, R. Johnson, S. Braun, J. Simpson, and P.E. Ciesielski, 2003b: Convective systems over the South China Sea: Cloud resolving model simulations. *J. Atmos. Sci.*, **60**, 2929-2956.

Tao, W.-K., D. Johnson, C.-L. Shie, and J. Simpson. 2004: Atmospheric energy budget and large-scale precipitation efficiency of convective systems during TOGA COARE, GATE, SCSMEX and ARM: Cloud-resolving model simulations, *J. Atmos. Sci.*, **61**, 2405-2423.

Tao, W.-K., S. Lang, X. Zeng, S. Shige, and Y. Takayabu, 2010: Relating convective and stratiform rain to latent heating, *J. Climate*, **23**, 1874-1893.

Tao, W.-K., E. Smith, R. Adler, Z. Haddad, A. Hou, T. Iguchi, R. Kakar, T.N. Krishnamurti, C. Kummerow, S. Lang, R. Meneghini, N. Nakamura, T. Nakazawa, K. Okamoto, W. Olson, S. Satoh, S. Shige, J. Simpson, Y. Takayabu, G. Tripoli, and S. Yang, 2006: Retrieval of latent heating from TRMM measurements, *Bull. Amer. Meteor. Soc.*, **87,** 1555-1572.

Tao, W.-K., Y. N. Takayabu, S. Lang, S. Shige, W. Olson, A. Hou, X. Jiang, C. Zhang, W. Lau, T. Krishnamurti, D. Waliser, M. Grecu, P. Ciesielski, R. Johnson, R. Houze, R. Kakar, N. Nakamura, S. Braun, S. Hagos, R. Oki, and A. Bhardwaj, 2016: TRMM latent heating retrieval: Applications and comparisons with field campaigns and large-scale analyses, *AMS Meteorological Monographs - Multi-scale Convection-Coupled Systems in the Tropics* (in press).

Zeng, X., W.-K. Tao, M. Zhang, S. Lang, C. Peters-Lidard, J. Simpson, S. Xie, S. Kumar, J. V. Geiger, C.-L. Shie, and J. L.. Eastman, 2007: Evaluation of long-term cloud-resolving modeling with observational cloud data. *J. Atmos. Sci.*, **64**, 4153-4177.

Zeng, X., W.-K. Tao, S. Lang, A. Hou, M. Zhang, and J. Simpson, 2008: On the sensitivity of Atmospheric ensemble to cloud microphysics in long-term cloud-resolving model simulations. *J. Meteor. Soc. Japan*, *Special Issue on high-resolution cloud models*, **86A**, 45-65.

Zeng, X., W.-K. Tao, M. Zhang, A. Y. Hou, S. Xie, S. Lang, X. Li, D. Starr, and X. Li, 2009: A contribution by ice nuclei to global warming. *Q. J. R. Met. Soc*., **135**, 1614-1629, DOI: 10.1002/qj.449.

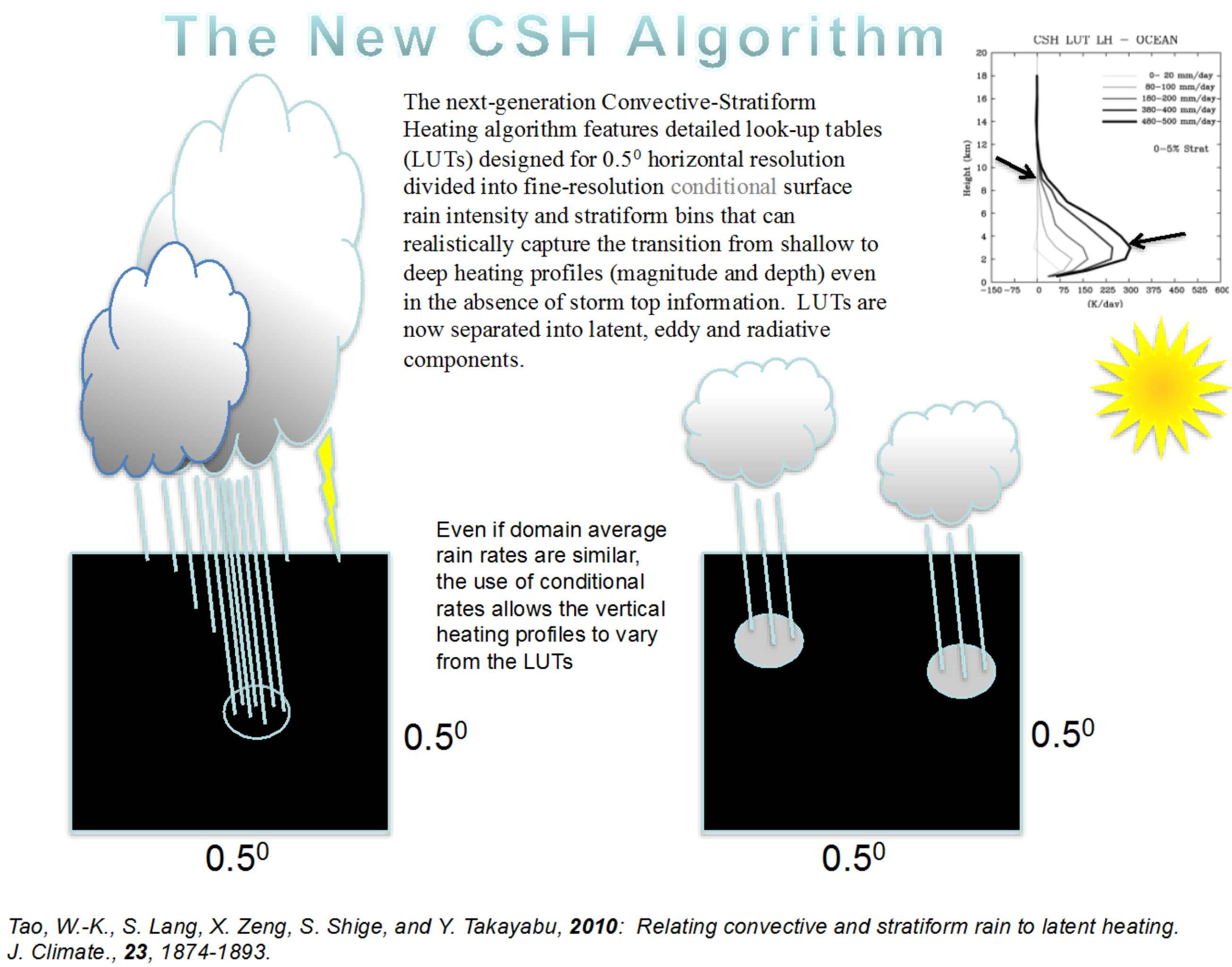

FIGURE 1 Schematic diagram showing the use of condition rain intensities rather than average rain intensities over a given domain. Using the conditional rain intensities allows for a better characterization of the rain. In the above example, the average rain intensities over each entire grid can be the same, but the conditional rain intensity is much higher for the grid on the left and would typically be associated with deeper convection.

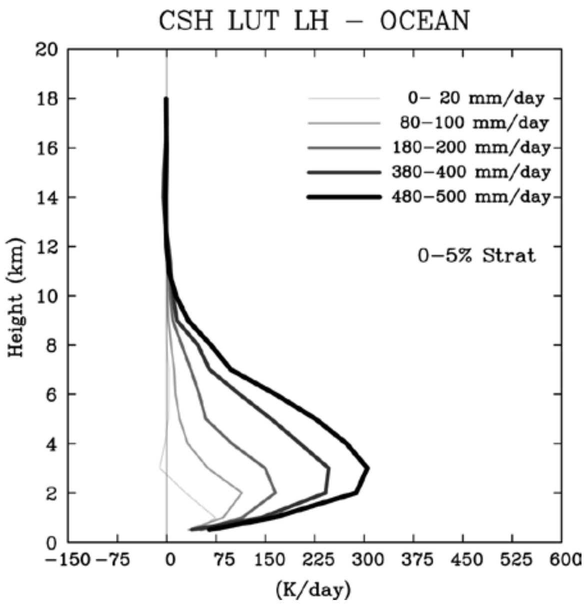

FIGURE 2 Sample CSH oceanic LUT profiles as a function of rain intensity for the most convective bin (i.e., having a stratiform % of 0 to 5%, left panel) and sample CSH oceanic LUT profiles as a function of stratiform fraction at a constant conditional rain intensity bin (i.e., 140 to 160 mm/day, right panel). After selecting the appropriate profiles based on the conditional surface rain intensity, the final heating profile is then adjusted according to the average rainfall.